

# Performance of Hybrid Neuro-Fuzzy Model for Solar Radiation Simulation at Abuja, Nigeria: A Correlation Based Input Selection Technique

Otitodilichukwu Excel Omeje<sup>1</sup>, Bara'u Gafai Najashi<sup>2</sup>, Hamza Sabo Maccido<sup>2</sup>, Yusuf Abdullahi Badamasi<sup>2</sup>, S.I. Abba<sup>3,\*</sup>

<sup>1</sup> Department of Electrical and Electronic Engineering, University of Abuja, Nigeria; titooomeje@gmail.com

<sup>2</sup> Department of Electrical and Electronic Engineering, Baze University Abuja, Nigeria; najashi.gafai@bazeuniversity.edu.ng; hamza.maccido@bazeuniversity.edu.ng; yusuf.abdullahi@bazeuniversity.edu.ng

<sup>3</sup> Department of Civil Engineering, Baze University Abuja, Nigeria

\* Correspondence: sani.abba@bazeuniversity.edu.ng

Manuscript received: 19-09-2021, revised: 20-11-2021, accepted: 03-12-2021.

## Abstract

Solar Radiation (Rs) simulations for specific locations are critical for guiding decisions about the design and operation of solar energy conversion devices. The expensive instruments required to make high-resolution Rs measurements, as well as the rigorous maintenance procedures connected with such devices, limit Rs measurements. As a result, the ability to simulate Rs using easily observed environmental data is essential (such as temperature, humidity, cloud cover, etc.). This study looks at how well a machine learning model called Adaptive Neuro-Fuzzy Inference System (ANFIS) performs in estimating Rs in Abuja, Nigeria. Monthly maximum and minimum temperatures, relative and specific humidity, precipitation, and surface pressure data were collected. Four different statistical metrics ( $R^2$ , R, MSE, RMSE) are considered to evaluate the performance of this model. Best results were produced from a parameter combination of minimum temperature, precipitation, and surface pressure with  $R^2$  of 0.8914 and RMSE of 0.0550 in the training phase and  $R^2$  of 0.9744, and RMSE of 0.0444 in the testing phase. The results show that the hybrid model, ANFIS, is highly efficient in forecasting Rs in Abuja.

**Keywords:** Adaptive neuro-fuzzy inference system; simulation; solar radiation; Nigeria.

## 1. Introduction

Several radiometers, such as the Pyranometer, Albedometer, Pyrheliometer, and others, are used to measure solar radiation [1]. However, these instruments are expensive to purchase and maintain, and they require rigorous calibration regularly [2]. This restricts Rs measurement, particularly in developing nations within Africa [3]. This is why it is critical to be able to simulate or predict Rs using easily observed environmental data (such as temperature, humidity, cloud cover, wind speed, and so on). Artificial Intelligence (AI) has gained significance in practically every engineering discipline as a result of technological breakthroughs in recent decades [4]. Machine Learning (ML), a subset of artificial intelligence, has been used to forecast Rs data, and previous studies have shown that ML models are very accurate in forecasting Rs [5]–[7].

Some of these ML models are Artificial Neural Networks (ANN), Support Vector Machine (SVM), Genetic Algorithms (GA), Deep Learning (DL), Kernel Nearest Neighbour (KNN), etc. Tymvios et al. compared ANN-type models with Angstrom's empirical models to forecast global solar radiation, their results showed that ANN models produced better forecasts than Angstrom-type models [8]. Kaba et al. used a deep learning method to estimate Rs for several locations in Turkey; In their study, parameters such as sunshine duration, cloud cover, minimum and maximum temperature were used to train the DL algorithm. The best results yielded a coefficient of determination ( $R^2$ ) value of 0.98 [9]. Another study by Meenal and Selvakumar forecasted daily global Rs with empirical, SVM and ANN models in India; the best results were produced by the SVM model with a correlation greater than 0.99 [10]. In China, Wang et al. compared three ANN-type models, Multilayer Perceptron (MLP), Generalized Regression Neural Network (GRNN), and Radial Basis Neural Network (RBNN) with empirical models in forecasting solar radiation. At different stations, it was observed that the models exhibited contrasting performance, yet the ANN model produced better forecasts than the empirical models [11]. In Australia, Doe et al. adopted SVM, coupled with wavelet transform to develop a

hybrid model for modelling solar radiation; from their study, they showed that the coupled method produced better  $R_s$  forecasts than the original SVM model [12].

Similarly, Hassan et al. examined the potential of three ML algorithms namely ANFIS, SVM, and MLP in forecasting  $R_s$  coming unto the horizontal surface. In their study, the best results were obtained from the MLP model, followed by ANFIS and SVM models [13]. Govindasamy and Chetty studied the effectiveness of using ANN, GRNN, Support Vector Regression (SVR), and Random Forest (RF) for  $R_s$  forecasting across South Africa, ANN models yielded the best results with high correlation coefficients and minimal errors in the forecasts [14]. Marzouq et al. compared the results of a proposed hybrid model (KNN and ANN) with an empirical model to forecast daily  $R_s$  in Morocco; best results were obtained from the hybrid model with an  $R^2$  value of 0.97 [15]. In the United Arab Emirates, Hussain and AlAlihi proposed a hybrid model of four different ANN-type architectures; GRNN, MLP, Adaptive Neuro-Fuzzy Inference System (ANFIS), and Nonlinear Autoregressive Recurrent Exogenous Neural Network (NARX) for forecasting solar radiation. This hybrid technique presented an improvement in the results of ANN models [16].

Nigeria is not left out in this trend as a couple of indigenous ML engineers have employed ML models to forecast  $R_s$  across different locations in Nigeria. Olatomiwa et al. developed a hybrid model of SVM and firefly algorithm (FFA) to forecast the monthly mean horizontal global  $R_s$  in Jos, Iseyin, and Maiduguri. The accuracy of this novel model was examined over various standard metrics and the results proved that the model provided better forecasts than that of ANN and GA models [17]. Another study by Kuhe et al. used RBNN, GRNN, and Feed-Forward Back-Propagation Neural Network (FFNN) to forecast the  $R_s$  in Makurdi; using ANN's ensemble, the results yielded forecasts with improved accuracy [18]. Salisu et al. evaluated the efficacy of two-hybrid approaches in forecasting  $R_s$  coming unto the horizontal surface in Kano; ANFIS was combined with Wavelet Transform (WT) and Particle Swarm Optimization (PSO) algorithms. The WT-ANFIS pair produced more accurate results than the PSO-ANFIS pair [19].

In Sokoto, Auwal et al. compared the performance of autoregressive-moving-average with exogenous inputs (ARMAX) and ANFIS in forecasting SR; their results showed that the ANFIS model with a Mean Absolute Percentage Error (MAPE) of 5.34% was a better model than ARMAX [20]. However, ML approaches for simulating  $R_s$  in Nigeria have not been adequately explored with very little published work using Abuja as a case study. This study aims to fill in this gap by analyzing the efficiency of the ANFIS model in simulating  $R_s$  in Abuja, Nigeria. The main objective of this work is (i) to conduct a correlation analysis to ascertain the key parameters required to forecast  $R_s$  more accurately (ii) to apply a hybrid ML model, ANFIS in forecasting daily  $R_s$  (iii) to evaluate the results obtained from ANFIS by using four metrics  $R^2$ , R, RMSE, and MSE. The driving force for this study is to provide useful  $R_s$  data and a model for monitoring the variability of  $R_s$  in Abuja, which is not only important for the design of a solar power plant but also for the sustained operation and management of such systems. This is to encourage the emergence of more solar power plants in Abuja, Nigeria.

## 2. Case Study and Dataset

The case study Abuja is Nigeria's capital and eighth-most populous city, situated at the centre of the nation, within the Federal Capital Territory (FCT) [21]. It has a longitude and latitude of  $9.0765^\circ$  N and  $7.3986^\circ$  E respectively, an elevation of 405m, and a total area of 1,769 km<sup>2</sup>. Abuja has an average daily global horizontal irradiation of 5.14 kWh/m<sup>2</sup> [22]. Figure 1 shows the location of the study area in the annual global  $R_s$  distribution map of Nigeria. Monthly measured climatic parameters such as maximum and minimum temperatures ( $T_{\max}$  and  $T_{\min}$  respectively), Relative Humidity (Hr), Specific Humidity (Hs), Precipitation (Pc), Surface Pressure (Ps), and  $R_s$  on a horizontal surface for a period of thirty-five years, ranging from January 1984 - December 2021, were retrieved from National Aeronautics and Space Administration (NASA) Prediction of Worldwide Energy Resources (POWER) Data Access Viewer. Data quality control was carried out on the data for cases where the variable was missing. The mean monthly variations of  $T_{\max}$ ,  $T_{\min}$ , Hr, Hs, Pc, Ps, and  $R_s$  are shown in Figure 2, it can be seen that an increase in Hr, Pc, Ps, and Hs in the rainy season (from April to October) leads to a decrease in  $T_{\max}$ ,  $T_{\min}$ , and  $R_s$ .  $R_s$  is highest in February and March and lowest in August.

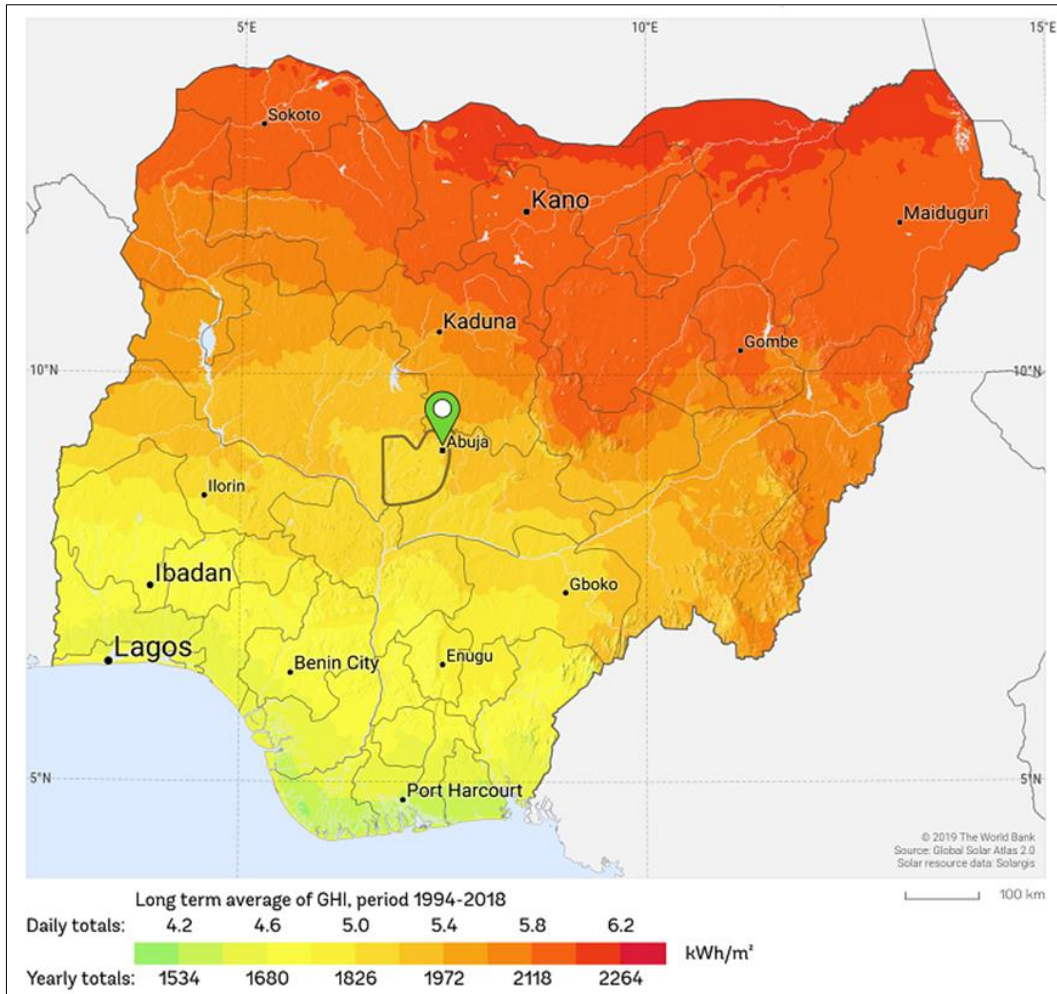
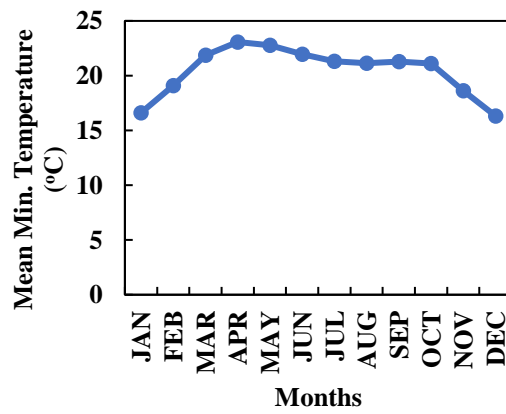
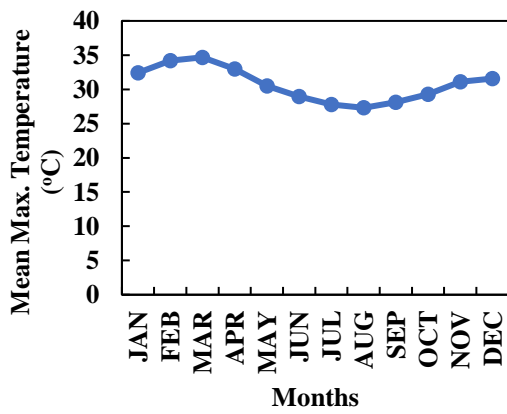


Figure 1. The annual global Rs distribution of Nigeria [23].



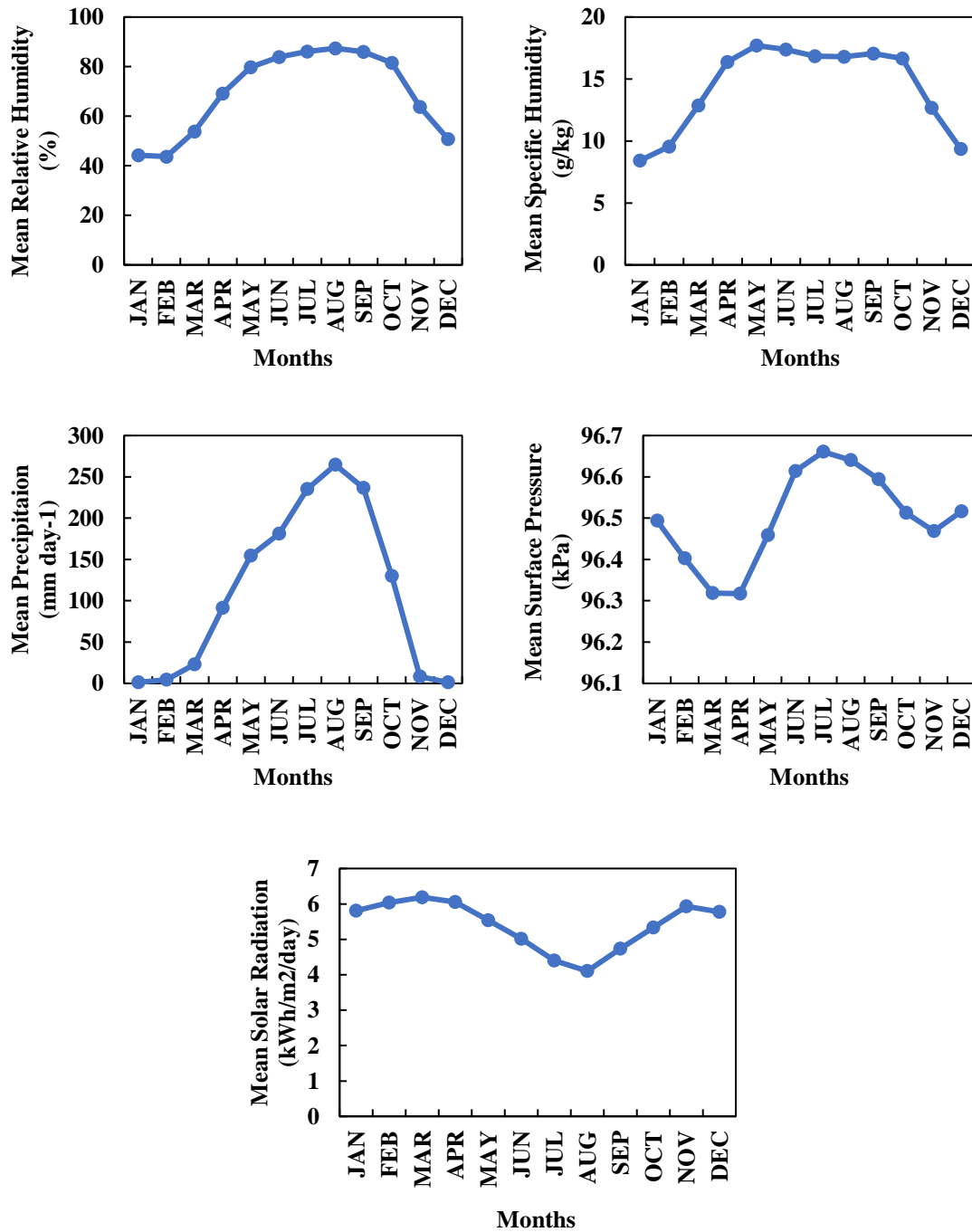


Figure 2. Mean monthly variations of individual parameters in the dataset.

### 3. Materials and Methods

#### 3.1. Adaptive Neuro-Fuzzy Inference System (ANFIS)

The neuro-fuzzy network is a five-layer feed-forward network that maps an input space to an output space using neural network learning algorithms and fuzzy reasoning. Figure 3 depicts the ANFIS architecture, and the following is a description of the model [22]–[24]. ANFIS has the ability to overcome the limitations of fuzzy inference and ANN. ANFIS model combines the ability of both ANN and Fuzzy logic to create a process that has the ability of handling complex non-linear interactions between a set of input and output [25]–[27].

**Layer 1:** In this layer, each node adapts to a function parameter. The result from each node is a degree of membership value, which is determined by the membership functions' input. For instance, the membership

function can be either a gaussian membership function (1), a generalized bell membership function (2), or another type of membership function that can be used.

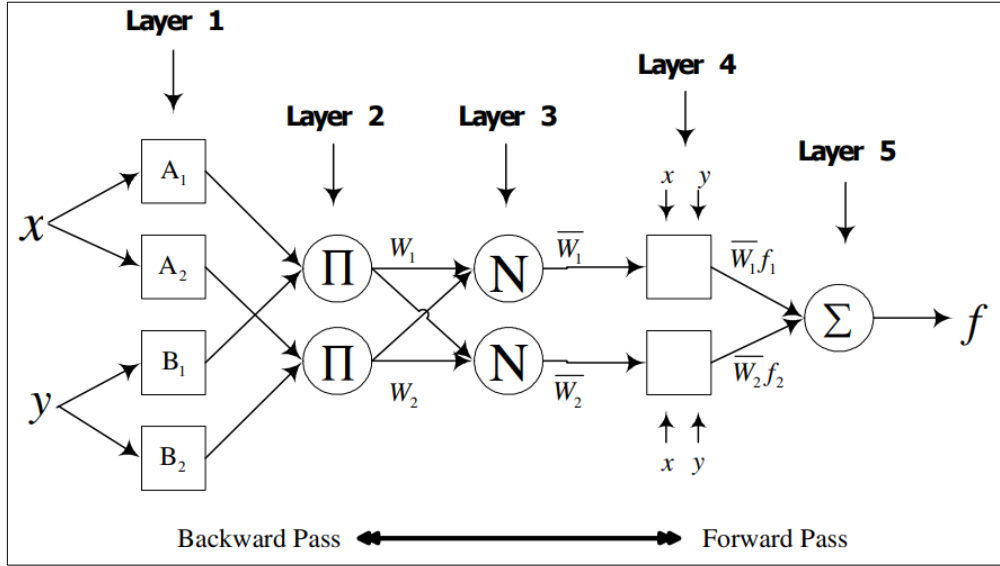


Figure 3. ANFIS architecture [25].

$$\mu_{A_i}(x) = \exp \left[ -\left( \frac{x - c_i}{2a_i} \right)^2 \right] \quad (1)$$

$$\mu_{A_i}(x) = \frac{1}{1 + \left| \frac{x - c_i}{a_i} \right|^{2b}} \quad (2)$$

$$O_{1,i} = \mu_{A_i}(x), \quad i = 1,2 \quad (3)$$

$$O_{1,i} = \mu_{B_{i-2}}(y), \quad i = 3,4 \quad (4)$$

where  $\mu_{A_i}$  and  $\mu_{B_{i-2}}$  are the degree of membership functions for the fuzzy sets  $A_i$  and  $B_i$  respectively, and  $\{a_i, b_i, c_i\}$  are the parameters of a membership function that can change the shape of the membership function. Premise parameters are the terms used to describe the parameters in this layer.

**Layer 2:** Every node in this layer is fixed or nonadaptive, and the circle node is labeled as Π. The output node is the result of multiplying the signal coming into the node and delivered to the next node. Each node in this layer represents the firing strength for each rule. In the second layer, the T-norm operator with general performance, such as the AND, is applied to obtain the output [28];

$$O_{2i} = w_i = \mu_{A_i}(x) * \mu_{B_i}(y), \quad i = 1,2 \quad (5)$$

where  $w_i$  is the output that represents the firing strength of each rule.

**Layer 3:** This layer's nodes are either fixed or nonadaptive, with the circle node labelled as N. The ratio between the  $i$ -th rule's firing strength and the sum of all rules' firing strengths is calculated at each node. The normalized firing strength is the name given to this result.

$$O_{3i} = \bar{w} = \frac{w_i}{w_1 + w_2} \quad i = 1,2 \quad (6)$$

**Layer 4:** In this layer, every node is an adaptive node to output, with a node function defined as;

$$O_{4i} = \underline{w}_i f_i = \underline{w}_i (p_i x + q_i y + r_i) \quad (7)$$

where  $\underline{w}_i$  is the normalized firing strength from the previous layer (third layer) and  $(p_i x + q_i y + r_i)$  is a parameter in the node. Consequent parameters refer to the parameters in this layer.

**Layer 5:** This layer's single node is a fixed or nonadaptive node that sums all incoming signals from the previous node to compute the overall output. A circle node is labelled as Σ in this layer.

$$O_{5i} = \sum_i w_i f_i = \frac{\sum_i w_i f_i}{\sum_i w_i} \tag{8}$$

### 3.2 Performance Evaluation Metrics

The accuracy of forecasting models is the most important element in determining their performance success. As a result, the generally used error metrics are used to evaluate the outputs of prediction models as well as to compare them to one another. Metrics such as coefficient of determination ( $R^2$ ), correlation coefficient ( $R$ ), mean square error (MSE) and root mean square error (RMSE) were used to compare the performance success of the forecasting models used in this study [29]–[32].

$$R^2 = 1 - \frac{\sum_i^n (x_i - y_i)^2}{\sum_i^n (x_i - \underline{x}_i)^2} \tag{9}$$

$$R = \sqrt{\left(1 - \frac{\sum_i^n (x_i - y_i)^2}{\sum_i^n (x_i - \underline{x}_i)^2}\right)} \tag{10}$$

$$MSE = \frac{1}{n} \sum_{i=1}^n (x_i - y_i)^2 \tag{11}$$

$$RMSE = \sqrt{\left(\frac{1}{n} \sum_{i=1}^n (x_i - y_i)^2\right)} \tag{12}$$

where  $x_i$  are values of the x-variable in a sample,  $y_i$  are values of the y-variable in a sample,  $\underline{x}_i$  is the mean of the values of the x-variable and  $n$  is the number of data points.

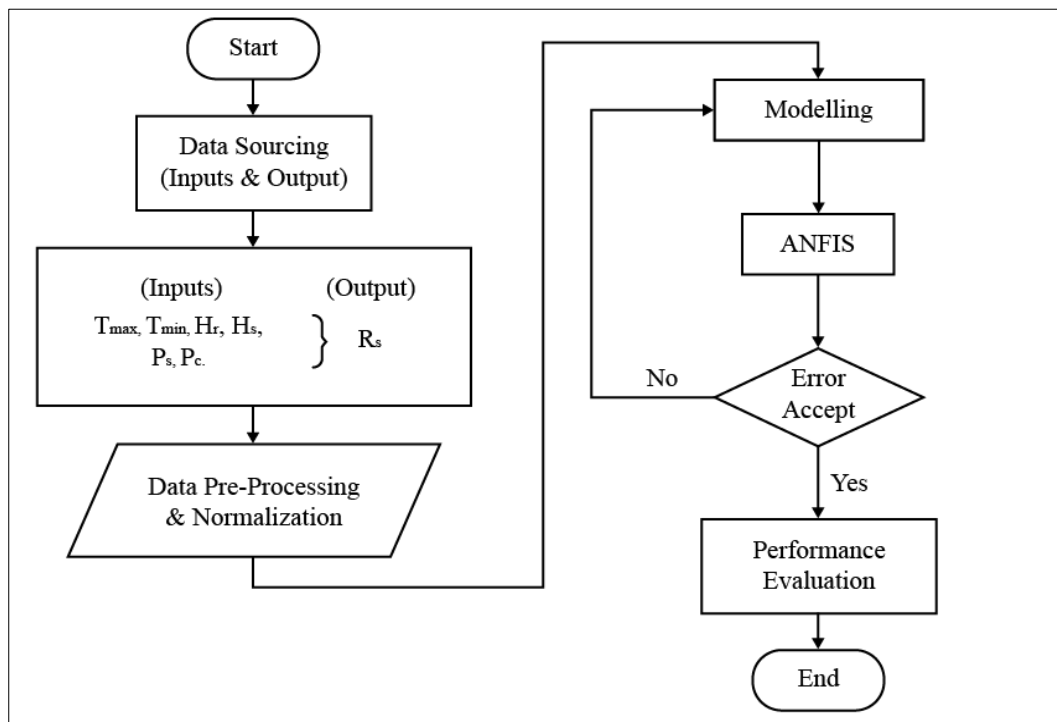


**Figure 4.** Forecasting solar radiation with ANFIS.

4. Results and discussions

4.1 Result for Correlation Analysis

The most dominant and suitable input combinations with the targeted variables were investigated using traditional sensitivity analysis and a correlation matrix. The type of linear relationship between the variables is represented by this matrix, see Figure 5. It can also be used as a basic indicator for the correlation of variable sets. From the sensitivity analysis done on the dataset used for this study; minimum and maximum temperatures, precipitation and surface pressure are key parameters required to accurately estimate solar radiation. The model combinations were generated based on the level of relationship between each variable and solar radiation,  $R_s$ .  $T_{min}$  has the highest relationship with a value of -0.57 while  $H_s$  has the lowest relationship with a value of 0.18. The generated models are M1, M2, M3, M4, M5 and M6, for use in both ANFIS and MLR models. An input/output combination of the normalized atmospheric variables and  $R_s$  was used for the modelling.

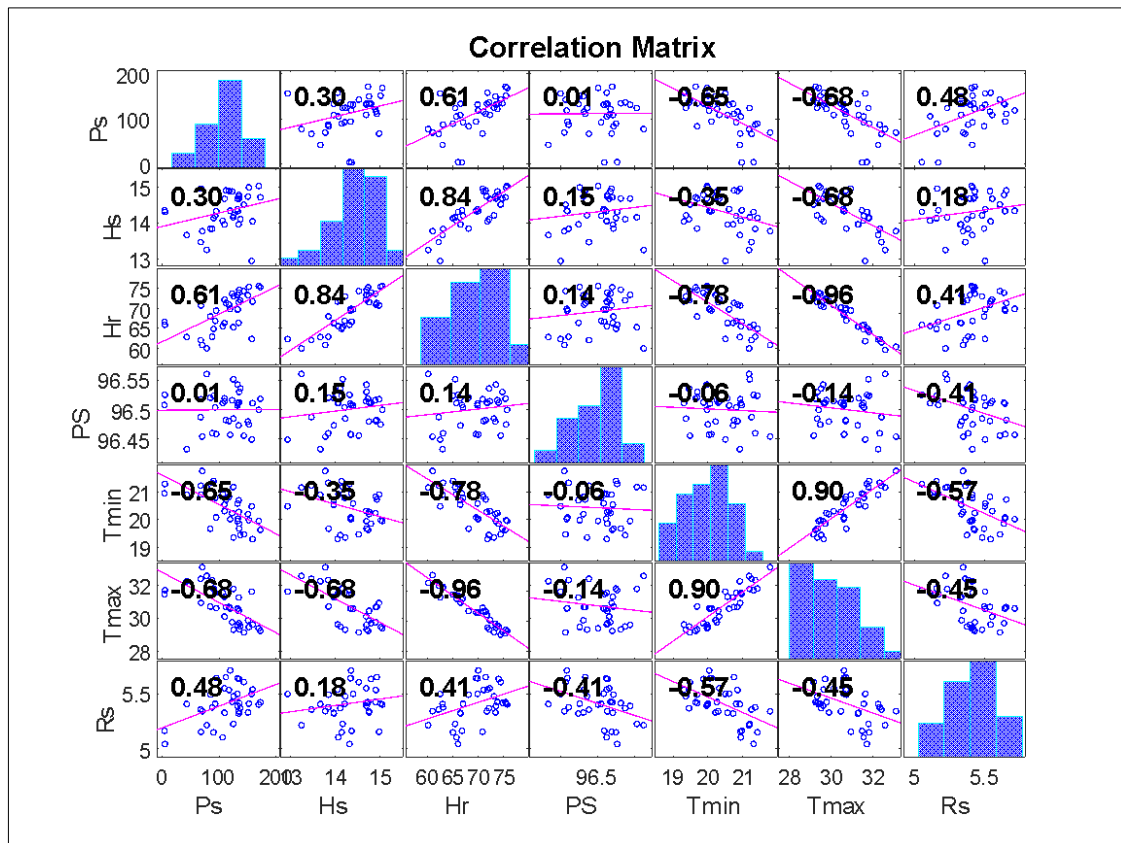


Figure 5. Correlation matrix between the experimental variables.

4.2 Result Analysis of ANFIS Model

The forecasted  $R_s$  values produced by the ANFIS model were partitioned into training (75%) and testing (25%) to properly evaluate the performance of ANFIS in forecasting solar radiation. The results of the performance criteria are displayed in Table 1. It can be seen that ANFIS-M4 with a parameter combination of minimum temperature, precipitation and surface pressure, produced the best training results with values of  $R^2 = 0.8914$ ,  $R = 0.9441$ ,  $MSE = 0.0030$ , and  $RMSE = 0.0550$  as well as the best testing results with  $R^2 = 0.9744$ ,  $R = 0.9871$ ,  $MSE = 0.0020$ , and  $RMSE = 0.0444$ . ANFIS-M2 with a parameter combination of minimum temperature and precipitation produced the worst training results of the ANFIS models with values of  $R^2 = 0.0497$ ,  $R = 0.2229$ ,  $MSE = 0.0265$ , and  $RMSE = 0.1627$ . While ANFIS-M1 produced the worst testing results with  $R^2 = 0.4857$ ,  $R = 0.6969$ ,  $MSE = 0.0396$ , and  $RMSE = 0.1990$ .

**Table 1.** Model performance and error statistics.

	TRAINING PHASE (75%)				TESTING PHASE (25%)			
	R <sup>2</sup>	R	MSE	RMSE	R <sup>2</sup>	R	MSE	RMSE
<b>ANFIS-M1</b>	0.2152	0.4639	0.0339	0.1840	0.4857	0.6969	0.0396	0.1990
<b>ANFIS-M2</b>	0.0497	0.2229	0.0265	0.1627	0.6601	0.8125	0.0262	0.1618
<b>ANFIS-M3</b>	0.6056	0.7782	0.0110	0.1048	0.9563	0.9779	0.0034	0.0580
<b>ANFIS-M4</b>	<b>0.8914</b>	<b>0.9441</b>	<b>0.0030</b>	<b>0.0550</b>	<b>0.9744</b>	<b>0.9871</b>	<b>0.0020</b>	<b>0.0444</b>
<b>ANFIS-M5</b>	0.5412	0.7357	0.0128	0.1131	0.9581	0.9788	0.0032	0.0568
<b>ANFIS-M6</b>	0.5495	0.7413	0.0125	0.1120	0.8710	0.9333	0.0099	0.0996

The results from ANFIS-M4 shows that the hybrid model is efficient in forecasting Rs in Abuja. This is justified by utilizing radar plots showing the R<sup>2</sup> and R values in both training and testing models for the ANFIS models in Figure 6. Radar plots, also known as spider plots, range from 0 to 1 are excellent for determining which variables in a dataset are scoring high or low, making them ideal for presenting performance.

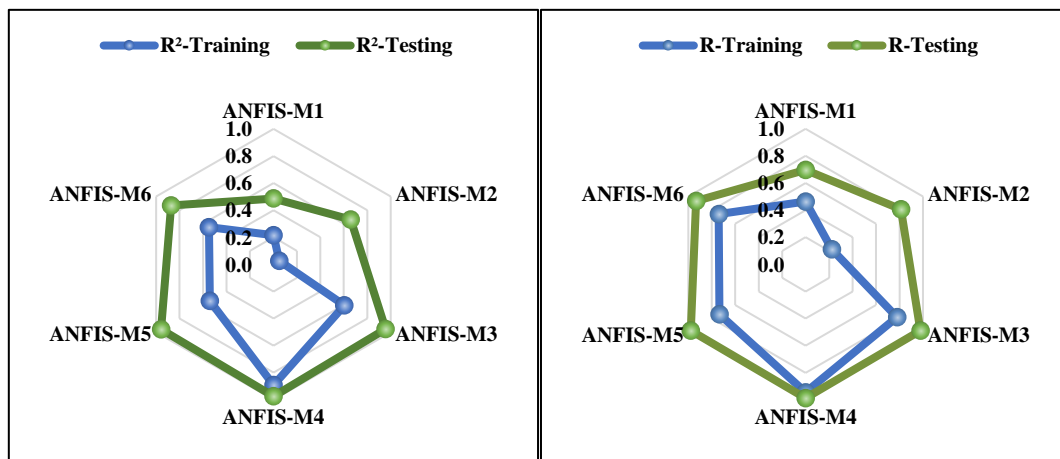


**Figure 6.** ANFIS radar plots for R<sup>2</sup> and R for both training and testing.

For additional understanding, the results produced by the best two models from ANFIS are analyzed using a time series plot to show how the observed Rs values and the forecasted Rs values vary concerning time in other words, the degree of agreement between the variables. When such variables in the plot overlap, that is the pattern of time variation between the variables are similar, such variables agree. The time series plot for the best ANFIS model (ANFIS-M4) is shown in Figure 7, while the time series plot for the second-best ANFIS model (ANFIS-M3) is shown in Figure 8. As shown in Figure 7 it can be seen that in ANFIS-M4, the predicted value nearly overlaps with the observed value; this implies that there is a higher degree of agreement between the observed and predicted values.



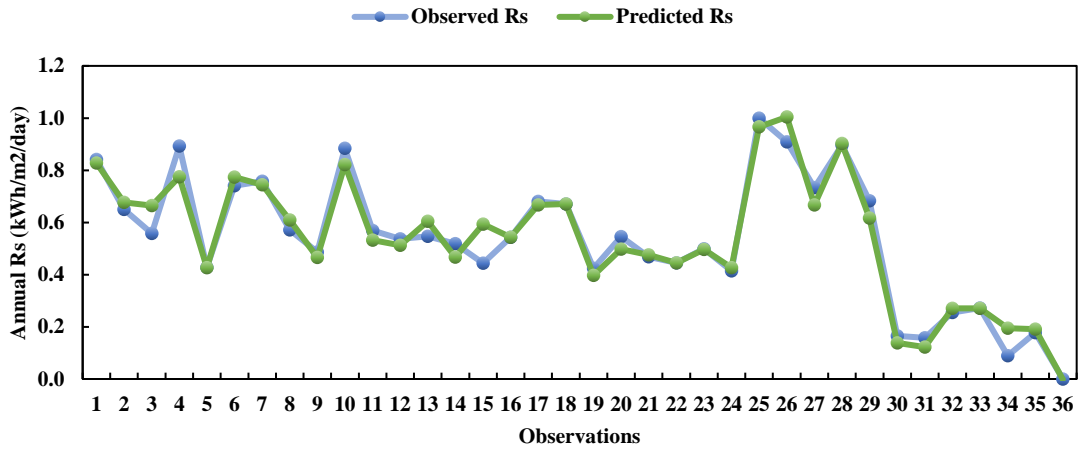


Figure 7. Time series plot for ANFIS-M4.

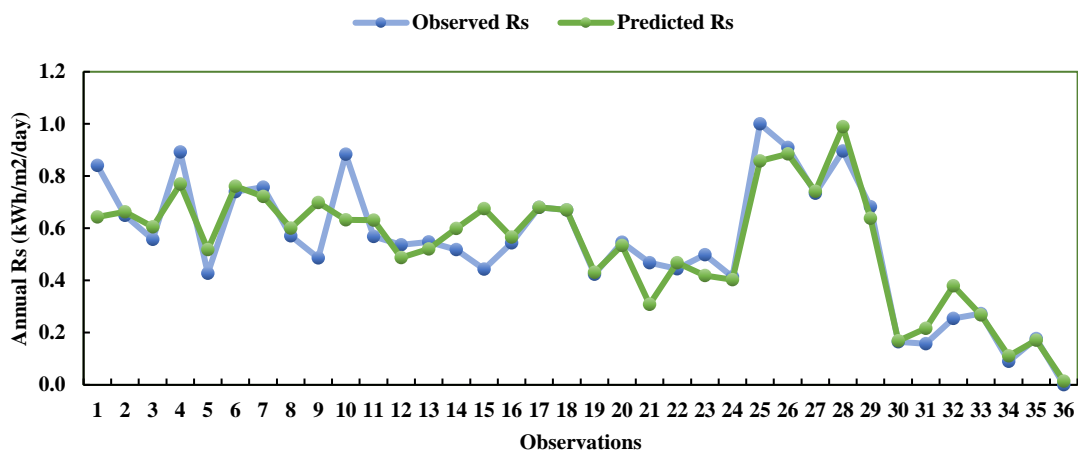


Figure 8. Time series plot for ANFIS-M3.

Figures 9 and 10 presented scatter plots that specifically present the results of the coefficient of determination ( $R^2$ ) and the agreement between observed and predicted values for the best two ANFIS models. The scatter plot is based on the equivalent average annual Rs of the dataset, to prevent overplotting of values. There is a greater level of agreement between the observed and predicted values in ANFIS-M4 than in ANFIS-M3 as the points become closely scattered around the trendline of ANFIS-M4.

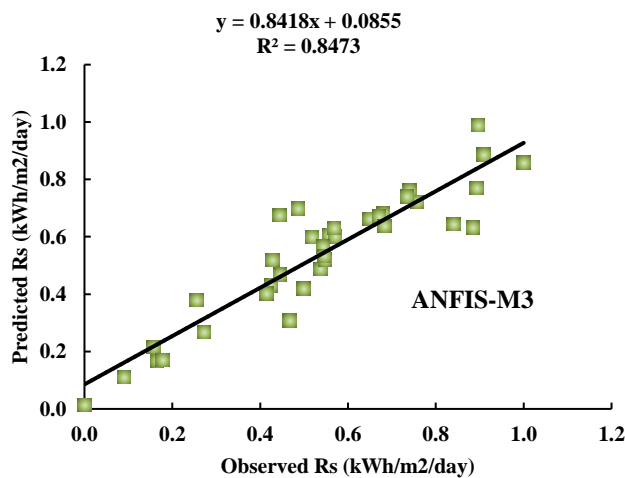
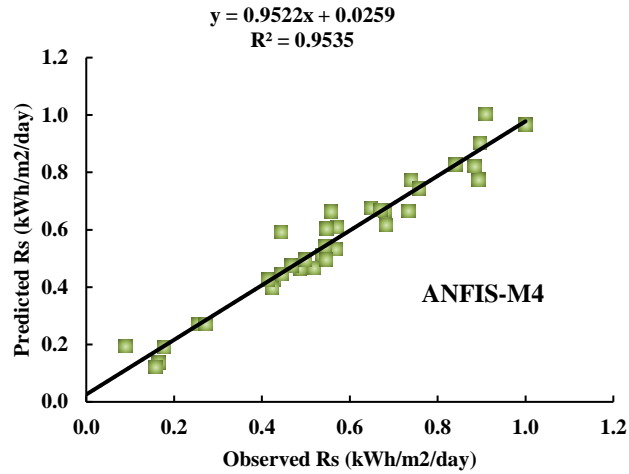
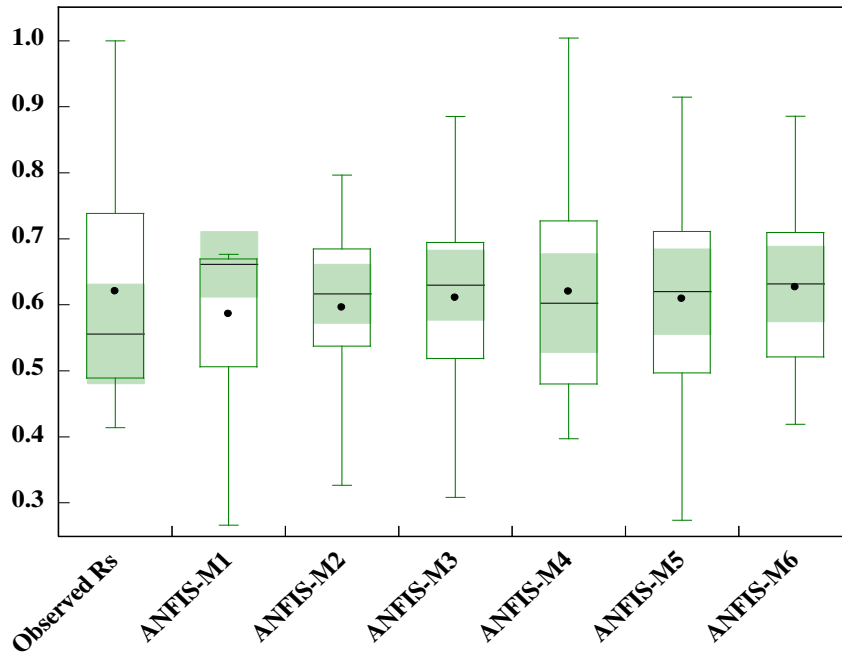


Figure 9. Scatter plots for ANFIS-M3.



**Figure 10.** Scatter plots for ANFIS-M4.

For further analysis of the results, box and whisker plots are introduced for the models. Box plots are a graphical representation that gives a statistical summary of a dataset. The box and whisker plots are characterized as effective condensed numerical tools for presenting data. The box plots indicate the proximity between the predicted and observed load. All ANFIS models were used for this analysis. For the training phase, based on the whiskers, mean, and median of the boxplot in Figure 11, it can be seen that ANFIS-M4 has the closest resemblance with that of the observed Rs values. For the testing phase, based on the whiskers, near outliers, mean, and median of the boxplot in Figure 12, ANFIS-M4 also has the closest appearance with that of the observed Rs values.



**Figure 11.** Training phase box plot between observed and predicted solar radiation for ANFIS.

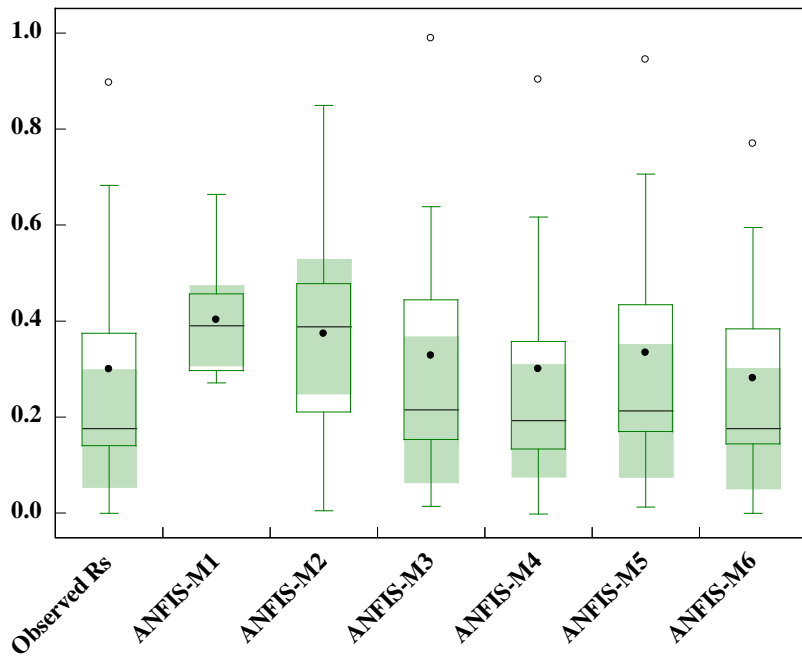


**Figure 12.** Testing phase box plot between observed and predicted solar radiation for ANFIS.

For more validation again the literature review, a bibliometric network based on the reported studies in the Scopus database (1999-2021) was visualized for an extensive literature review regarding the generalization of machine learning to handle chaotic SR prediction. Figure 13 shows that the SR prediction models using an AI-based approach are receiving a lot of attention. Over 300 clustered keywords and the probability of occurrences were presented, demonstrating the topic's weight and significance in SR prediction models. This simulation uses experimental data to create a prototype of a physical model to predict its performance in the real world with the help of scientific modeling of natural systems. This simulation can help with an appropriate decision by decision-makers and other stakeholders.

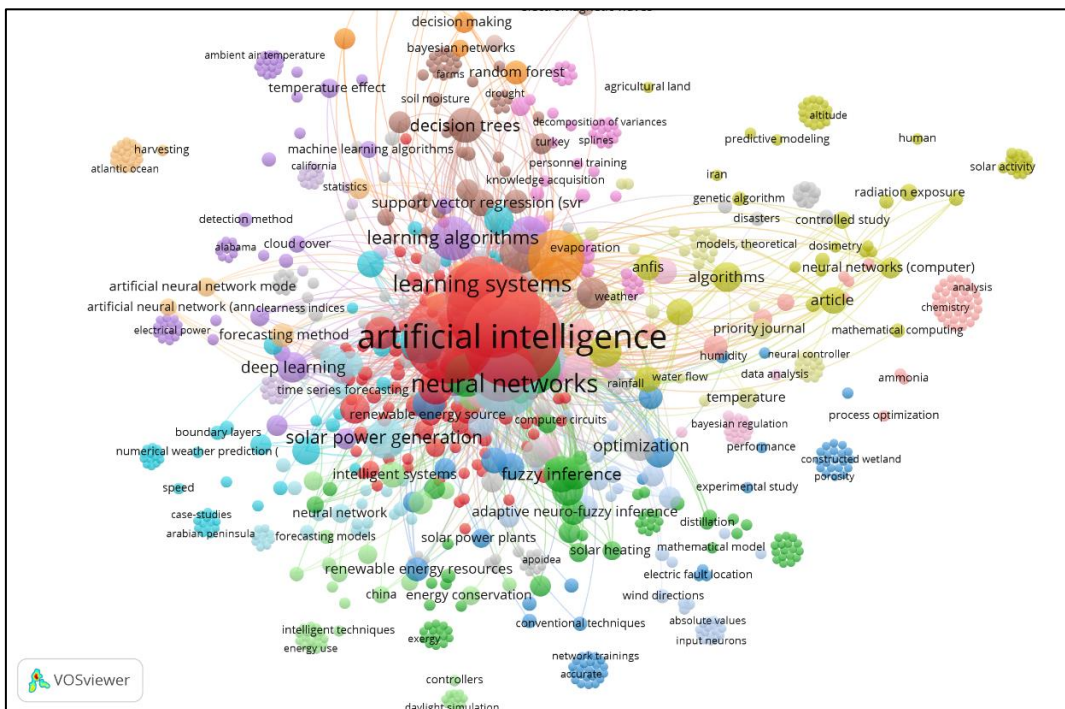


**Figure 13.** A bibliometric network on SR prediction models in Scopus database (1999-2021).

## 5. Conclusion

This study was conducted to analyse the performance accuracy of a hybrid ANFIS for forecasting Rs in Abuja, Nigeria. The motivation for this study is to provide useful Rs data and a model for monitoring the variability of Rs in Abuja, which is not only important for the design of a solar power plant but also for the sustained operation and management of such systems. This is to encourage the emergence of more solar power plants in Abuja, Nigeria. The idea was to use widely accessible measurable climatic parameters (maximum and minimum temperatures, relative humidity, specific humidity, precipitation, and surface pressure) as inputs to simulate Rs (the output). These input parameters were chosen because of their widespread availability for all locations, high correlations with solar radiation, and the ease with which they can be retrieved. This study which was based on long-term measured data retrieved from National Aeronautics and Space Administration (NASA) POWER Data Access Viewer, has led to the following conclusions:

- i. According to the statistical performance metrics obtained, simulating Rs using ANFIS produces results with a higher degree of reliability with  $R^2$  of 0.8914 and RMSE of 0.0550 than MLR with  $R^2$  of 0.6686 and RMSE of 0.1597.
- ii. Based on the correlation analysis done on the dataset used for this study: minimum and maximum temperatures, precipitation and surface pressure are key parameters required to accurately estimate solar radiation.
- iii. When dealing with a range of input parameters, the ANFIS model is observed to be both highly scalable and adaptable. As a result, the model may be used as a unit to predict Rs data based on other commonly known climatic parameters.

As a future investigation, the ANFIS model should be combined with other machine learning methods to improve its predictive accuracy. In addition, more climatic input parameters should be investigated.

**Acknowledgments:** The authors would like to appreciate the National Aeronautics and Space Administration (NASA) for the Prediction of Worldwide Energy Resources (POWER) project, which provided the data used to carry out this study. The authors would also like to appreciate the University of Abuja and Baze University for supporting this work.

**Conflicts of Interest:** No

## References

- [1] H. P. Garg and S. N. Garg, "Measurement of solar radiation. Pt. 1; Radiation instruments," *Renew. Energy;(United Kingdom)*, vol. 3, 1993.
- [2] Y. Feng, W. Hao, H. Li, N. Cui, D. Gong, and L. Gao, "Machine learning models to quantify and map daily global solar radiation and photovoltaic power," *Renew. Sustain. Energy Rev.*, 2020.
- [3] A. Sharafati *et al.*, "The potential of novel data mining models for global solar radiation prediction," *Int. J. Environ. Sci. Technol.*, no. 0123456789, 2019.
- [4] C. Huang, Z. Zhao, L. Wang, Z. Zhang, and X. Luo, "Point and interval forecasting of solar irradiance with an active Gaussian process," *IET Renew. Power Gener.*, vol. 14, no. 6, pp. 1020–1030, 2020.
- [5] V. H. Quej, J. Almorox, J. A. Arnaldo, and L. Saito, "ANFIS, SVM and ANN soft-computing techniques to estimate daily global solar radiation in a warm sub-humid environment," *J. Atmos. Solar-Terrestrial Phys.*, vol. 155, no. September 2016, pp. 62–70, 2017.
- [6] Y. Liu, Y. Zhou, Y. Chen, D. Wang, Y. Wang, and Y. Zhu, "Comparison of support vector machine and copula-based nonlinear quantile regression for estimating the daily diffuse solar radiation: A case study in China," *Renew. Energy*, vol. 146, pp. 1101–1112, 2020.
- [7] T. Hai *et al.*, "Global Solar Radiation Estimation and Climatic Variability Analysis Using Extreme Learning Machine Based Predictive Model," *IEEE Access*, vol. 8, pp. 12026–12042, 2020.
- [8] F. S. Tymvios, C. P. Jacovides, S. C. Michaelides, and C. Scouteli, "Comparative study of Ångström's and artificial neural networks' methodologies in estimating global solar radiation," *Sol. Energy*, vol. 78, no. 6, pp. 752–762, 2005.
- [9] K. Kaba, M. Sarıgül, M. Avcı, and H. M. Kandırmaz, "Estimation of daily global solar radiation using deep learning model," *Energy*, vol. 162, pp. 126–135, 2018.
- [10] R. Meenal and A. I. Selvakumar, "Assessment of SVM, empirical and ANN based solar radiation prediction models with most influencing input parameters," *Renew. Energy*, vol. 121, pp. 324–343, 2018.
- [11] L. Wang, O. Kisi, M. Zounemat-kermani, G. Ariel, Z. Zhu, and W. Gong, "Solar radiation prediction using different techniques : model evaluation and comparison," *Renew. Sustain. Energy Rev.*, 2016.
- [12] R. C. Deo, X. Wen, and F. Qi, "A wavelet-coupled support vector machine model for forecasting global incident solar radiation using limited meteorological dataset," *Appl. Energy*, vol. 168, pp. 568–593, 2016.
- [13] M. A. Hassan, A. Khalil, S. Kaseb, and M. A. Kassem, "Potential of four different machine-learning algorithms in

- modeling daily global solar radiation,” *Renew. Energy*, vol. 111, pp. 52–62, 2017.
- [14] T. R. Govindasamy and N. Chetty, “Machine learning models to quantify the influence of PM10 aerosol concentration on global solar radiation prediction in South Africa,” *Clean. Eng. Technol.*, vol. 2, no. November 2020, p. 100042, 2021.
- [15] M. Marzouq, Z. Bounoua, H. el fadili, A. Mechaqrane, K. Zenkouar, and Z. Lakhliai, “New daily global solar irradiation estimation model based on automatic selection of input parameters using evolutionary artificial neural networks,” *J. Clean. Prod.*, vol. 209, Oct. 2018.
- [16] S. Hussain and A. AlAlili, “A hybrid solar radiation modeling approach using wavelet multiresolution analysis and artificial neural networks,” *Appl. Energy*, vol. 208, no. September, pp. 540–550, 2017.
- [17] L. Olatomiwa, S. Mekhilef, S. Shamshirband, K. Mohammadi, D. Petković, and C. Sudheer, “A support vector machine-firefly algorithm-based model for global solar radiation prediction,” *Sol. Energy*, vol. 115, pp. 632–644, 2015.
- [18] A. Kuhe, V. T. Achirgbenda, and M. Agada, “Global solar radiation prediction for Makurdi, Nigeria, using neural networks ensemble,” *Energy Sources, Part A Recover. Util. Environ. Eff.*, vol. 43, no. 11, pp. 1373–1385, 2021.
- [19] S. Salisu, M. W. Mustafa, M. Mustapha, and O. O. Mohammed, “Solar radiation forecasting in Nigeria based on hybrid PSO-ANFIS and WT-ANFIS approach,” *Int. J. Electr. Comput. Eng.*, vol. 9, no. 5, pp. 3916–3926, 2019.
- [20] A. Muhammad *et al.*, “Forecasting of global solar radiation using ANFIS and armax techniques,” *IOP Conf. Ser. Mater. Sci. Eng.*, vol. 303, no. 1, 2018.
- [21] B. Musa, N. Yimen, S. I. Abba, H. H. Adun, and M. Dagbasi, “Multi-state load demand forecasting using hybridized support vector regression integrated with optimal design of off-grid energy Systems—a metaheuristic approach,” *Processes*, vol. 9, no. 7, 2021.
- [22] K. Mahmoud *et al.*, “Prediction of the effects of environmental factors towards COVID-19 outbreak using AI-based models,” *IAES Int. J. Artif. Intell.*, vol. 10, no. 1, pp. 35–42, 2021.
- [23] G. Elkiran, V. Nourani, and S. I. Abba, “Multi-step ahead modelling of river water quality parameters using ensemble artificial intelligence-based approach,” *J. Hydrol.*, vol. 577, no. July, p. 123962, 2019.
- [24] S. I. Abba, S. J. Hadi, and J. Abdullahi, “River water modelling prediction using multi-linear regression, artificial neural network, and adaptive neuro-fuzzy inference system techniques,” *Procedia Comput. Sci.*, vol. 120, pp. 75–82, 2017.
- [25] V. N. G. Elkiran, S. I. Abba, and J. Abdullahi, “Artificial intelligence-based approaches for multi-station modelling of dissolve oxygen in river,” vol. 4, no. 4, 2018.
- [26] B. Mohammadi *et al.*, “Adaptive neuro-fuzzy inference system coupled with shuffled frog leaping algorithm for predicting river streamflow time series,” *Hydrol. Sci. J.*, vol. 0, no. 0, p. 1, 2020.
- [27] M. Alas *et al.*, “Experimental Evaluation and Modeling of Polymer Nanocomposite Modified Asphalt Binder Using ANN and ANFIS,” vol. 32, no. 10, pp. 1–11, 2020.
- [28] A. Sharafati *et al.*, “Performance evaluation of sediment ejector efficiency using hybrid neuro-fuzzy models,” *Eng. Appl. Comput. Fluid Mech.*, vol. 15, no. 1, pp. 627–643, 2021.
- [29] A. G. Usman, S. Işık, and S. I. Abba, “A Novel Multi-model Data-Driven Ensemble Technique for the Prediction of Retention Factor in HPLC Method Development,” *Chromatographia*, vol. 83, no. 8, pp. 933–945, 2020.
- [30] A. G. Usman, S. Işık, and S. I. Abba, “Hybrid data-intelligence algorithms for the simulation of thymoquinone in Hybrid data \_intelligence algorithms for the simulation of thymoquinone in HPLC method development,” *J. Iran. Chem. Soc.*, no. January, 2021.
- [31] S. I. Abba, A. G. Usman, and S. IŞIK, “Simulation for response surface in the HPLC optimization method development using artificial intelligence models: A data-driven approach,” *Chemom. Intell. Lab. Syst.*, vol. 201, no. April, 2020.
- [32] A. G. Usman, M. H. Ahmad, R. N. Danraka, and S. I. Abba, “The effect of ethanolic leaves extract of *Hymenodictyon floribundun* on inflammatory biomarkers: a data-driven approach,” *Bull. Natl. Res. Cent.*, vol. 45, no. 1, 2021.